INFLUENCE OF PREPARATION TEMPERATURES OF V_2O_5 POWDER ON REDUCTION RATE IN V_2O_5-SO_2 SYSTEM

Akira SHIMIZU, Shuji KAWARAI*, Ryusaburo FURUICHI and Tadao ISHII

(Received June 30, 1987)

Abstract

Reactivity of three V_2O_5 (**V1**, **V2** and **V3**) obtained at different preparation temperatures (T_p) was compared by their rate of reduction in SO_2 stream of 300 *ml/min*. The V_2O_5 samples were prepared by thermal decomposition of NH_4VO_3 in an air stream of 100 *ml/min* at 400 (**V1**), 450 (**V2**) and 550 °C (**V3**) for 1 *hr*. The reduction followed Mampel's equation in a temperature range of 350-400°*C*. The measured rate was decreased with an increase in T_p. SEM observation and measurements of interplanar spacing (d_{hoo}), peak breadth at half maximum intensity (β_{hoo}), BET surface area (S), and stretching vibration frequency of V=O(ν) of V_2O_5 were carried out. Values of ν and d_{hoo} were independent of T_p. Lattice strain η_a and crystallite size L_a were estimated by Hall's method from β_{hoo}. η_a was decreased with T_p while L_a was increased. L_a agreed with the diameter (D_s) calculated from S. The reduction was presumed to proceed on the surface of V_2O_5 crystallites. The change in the reduction rate with T_p was considered to depend on the strain energy stored in the crystallite.

1. Introduction

In our previous paper[1] thermal decomposition process of NH_4VO_3 was studied by gas flow DTA and X-ray technique. It was reported that a single phase of V_2O_5 crystal was obtained above 400°*C* and its crystal growth continued extensively up to 550°*C*. Since the crystallinity of V_2O_5 was affected by the decomposition temperature of NH_4VO_3 namely the preparation temperature of the oxide, it was assumed that the reactivity of V_2O_5 is affected by its preparation temperature. In the present investigation, three V_2O_5 samples were prepared at 400, 450 and 550 °*C* by thermal decomposition of NH_4VO_3. The changes in the reactivity of these V_2O_5 powders was investigated on the basis of the formation rate of V_4O_9, which is considered to have the closest resembling structure to that of V_2O_5 among all intermediate oxides formed in the course of the reduction of V_2O_5 with SO_2[2,3].

2. Experimental

2.1 Material

Three V_2O_5 (**V1**, **V2** and **V3**) samples were prepared by thermal decomposition of NH_4

Department of Applied Chemistry, Faculty of Engineering Hokkaido University *Hokkaido Gas Co. Ltd.

VO_3 (-250 *mesh*)[1]. A commercial NH_4VO_3 ($2g$) (Kanto Chemical Co. Reagent Grade) was heated in a horizontal electric furnace with a quartz tube ($\phi = 10$ *mm*) at an air flow rate of 100 *ml/min* for 1 *hr* at 400 (**V1**), 450 (**V2**) and 550 °*C* (**V3**), respectively. X-ray diffraction patterns of these V_2O_5 coincided with ASTM card[4]. SEM photographs of these samples are shown in Fig. 1. Particle size distribution of the samples were in the range of 1 to 10 μm and showed no relation to the preparation temperatures.

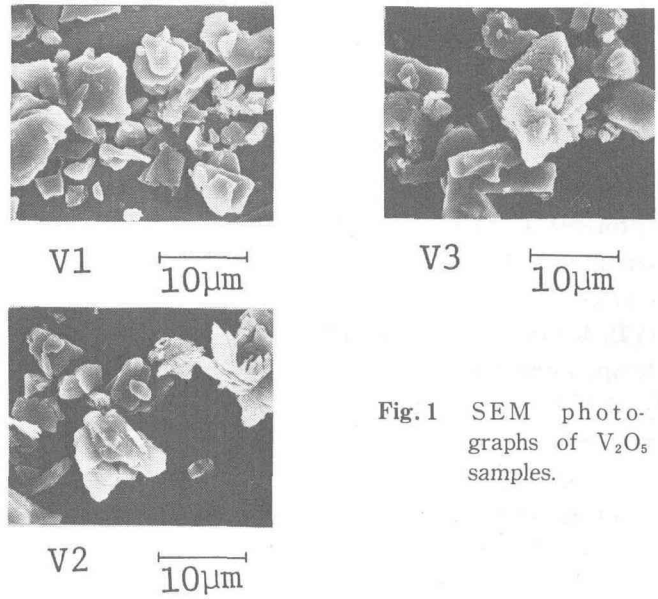

Fig. 1 SEM photographs of V_2O_5 samples.

2.2 Reaction method

The reduction of V_2O_5 sample (100 *mg*) was carried out in the quartz reaction tube ($\phi = 10$ *mm*) placed in a vertical electric furnace. The sample powder was supported by spreading it on a quartz wool layer packed in the tube. SO_2 gas was introduced at a constant flow rate into the reaction tube from a gas bomb (purity : 99.1 %). The gas was dried by passing the gas through a drying agent (P_2O_5). The fractions of V_2O_5 reduced (α) were 0.07, 0.23, 0.21 and 0.22 when sample **V2** was reduced at 400 °*C* for 2 *hr* under SO_2-flow rates of 100, 200, 300 and 400 *ml/min*, respectively. These α-values show that the effect of laminar film between gas and particle is constant over a flow rate of 200 *ml/min*. Accordingly, subsequent experiments were carried out at SO_2 flow rate of 300 *ml/min*. X-ray diffraction patterns of the mixed phase of V_2O_5 and V_4O_9 was obtained after the reduction of V_2O_5 samples for 5 *hr* in a temperature range of 350-400 °*C*. This fact is consistent with the result reported by Taniguchi et al[2]. for the formation temperature of V_4O_9 (320-430 °*C*). Then the reduction was carried out for 1 to 5 *hr* at the temperatures of 350, 375 and 400 °*C*.

2.3 Measurment of fractional conversion (α)

In order to determine the fraction of V_2O_5 reduced (α), the concentration ratio of vanadium ions, $[V^{4+}]/\{[V^{4+}]+[V^{5+}]\}$ was measured according to JIS[6] by means of potentiometric titration of Mohr's salt solution. After the reaction for a fixed time, 50 *mg*

of sample was dissolved in 100 *ml* of *3N*-H_2SO_4. The 10 *ml* of this solution was mixed with 10 *ml* of conc. H_3PO_4 and diluted to 100 *ml* with water and then titrated by 1/30*N*-Mohr's salt solution. The titration volume was represented by V_1 (*ml*). After the titration, V^{4+} ion in the solution was oxidized into V^{5+} by *0.1N*-$KMnO_4$. The solution was titrated once again by the Mohr's salt solution. This second titration volume was represented by V_2 (*ml*). Since V_2-V_1 is equivalent to the $[V^{4+}]$ and the reduction process is formulated as eq. (1),

$$2V_2O_5 + SO_2 \longrightarrow V_4O_9 + SO_3 \quad (1)$$

the fractional conversion (α) is represented by

$$\alpha = 2(V_2 - V_1)/V_2 \quad (2)$$

2.4 X-ray diffraction

X-ray powder diffractometer (Rigakudenki Co. Type 2142) was used for identification of the samples before and after the reaction. The diffraction peak breadth at half-maximum intensity[7] and the interplanar spacing were measured from the diffraction peak profile. The profile was obtained by the manual step scan method. The scan was carried out by moving the gonimeter every 1/100 *degrees*. The diffraction intensities were counted five times for 10 *sec* at the each angle. The standard sample of V_2O_5, which was prepared by calcining **V3** at 650 °*C* for 24 *hr* in air, and that of α-Al_2O_3, which was prepared by calcining activated alumina at 1300 °C for 3 *hr*, were used for the estimation of the peak breadth and the interplanar spacing, respectively. Cu-target was used in the former case and Cr-target in the latter.

2.5 IR measurment

The stretching vibration of V=0 group was measured by KBr disk method, using IR spectrometer (Shimazu Co. 430). The disk was prepared by pressing the mixture of 0.1 *mg* of sample and 200 *mg* of KBr powder at a pressure of 5.3 ton/cm^2.

2.6 SEM observation

The particle of samples was observed by SEM (JEOL T-20). The sample was dispersed in ethanol by ultrasonic wave generator and then sedimented on the sample holder (Aluminum disk $\phi = 15$ *mm*). The suface of the sample was coated with a gold film in vacuum evaporator to prevent electrification.

2.7 BET surface area measurment

The surface area was calculated by BET equation from the amount of adsorbed Ar at −197 °*C*. Before the adsorption, the sample (0.4*g*) was evacuated at 10^{-4} *mmHg* for 10 *hr* at room temperature.

3. Result and discussion

As shown in Fig. 2, the reduction rate of three V_2O_5 (**V1**, **V2** and **V3**) is found to follow Mampel's equation[8] (eq. (3)), which is based on an assumption that the rate controlling step is the phase-boundary reaction.

$$1-(1-\alpha)^{1/3} = k_M t \quad (3)$$

It may be observed from the slopes of the straight lines of Fig. 2 that the lower the preparation temperature of V_2O_5 is, the larger the k_M-value is. Table 1 shows the values of k_M and activation energies (E_a) of three V_2O_5. X-ray diffraction revealed that the samples obtained in the course of the reaction were a mixture of V_2O_5 and V_4O_9.

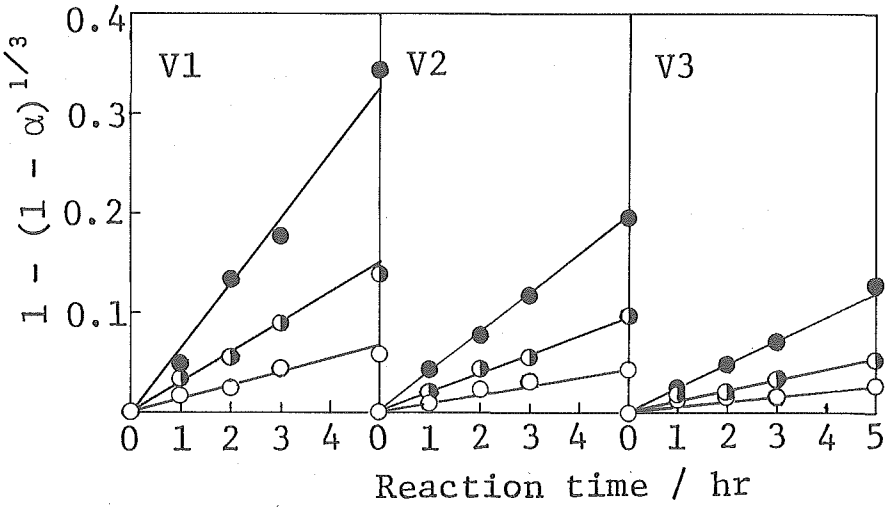

Fig. 2 Plots of $1-(1-\alpha)^{1/3}$ vs. time for reaction of V_2O_5 samples. Reaction temperature, ○: 350°C, ◑: 375°C, ●: 400°C.

Table 1 Reaction rate constants [k_M] and activation energies [E_a].

Sample	Reaction temperature/°C	k_M/hr^{-1}	$E_a/kcal\cdot mol^{-1}$
V1	350	1.36×10^{-2}	27
	375	3.00×10^{-2}	
	400	6.93×10^{-2}	
V2	350	9.20×10^{-3}	26
	375	1.90×10^{-2}	
	400	3.90×10^{-2}	
V3	350	5.60×10^{-3}	25
	375	1.02×10^{-2}	
	400	2.30×10^{-2}	

Table 2 Interplanar spacing [d_{hkl}], peak breadth at half-maximum intensity [β_{hkl}] and specific surface area [S].

Sample	**V1**	**V2**	**V3**
d_{hkl}/A			
d_{600}	1.918	1.918	1.918
d_{400}	2.883	2.883	2.883
d_{200}	5.773	5.773	5.774
β_{hkl}/deg			
β_{600}	0.097	0.057	0.038
β_{400}	0.075	0.045	0.032
β_{200}	0.057	0.030	0.021
$S/m^2\cdot g^{-1}$	7.4	5.6	3.5

Table 2 shows the interplanar spacing (d_{600}, d_{400} and d_{200}) and peak breadth at half maximum intensity (β_{600}, β_{400} and β_{200}) of three crystal faces aligned in the direction of a-axis, and specific surface areas (S). The difference in d_{hoo}-values is not observed between the samples. On the other hand, β_{hoo}-value decreases with an increase in the preparation temperature. It is suggested from the change in β_{hoo} that the crystallinity of V_2O_5 increases with its preparation temperature. The surface area (S) correspondingly decreases with the preparation temperature. From SEM photographs of **V3** in Fig. 1 and an assumption that the particle of sample is cubic, the average size of the particle was measured to be 5 μm, which lead to a calculation of the surface area of 0.35 m^2/g by using the density of V_2O_5 (3.4 g/cm^2). This is much smaller than the BET area of 3.5 m^2/g measured for **V3**. The discrepancy leads to a conclusion that every particle of the sample consists of many small particles. Fig. 3 shows the magnified SEM photographs of **V1**, **V2** and **V3**. It is observed that many smaller particles combine with each other and build up the large particles of the sample. Furthermore, the size of the smaller particle is observed to increase with the preparation temperature. The average size of the samller particle was estimated to be 5.2×10^3 A in the case of **V3** which shows the smaller particles most clearly.

From the BET specific surface area, the particle diameter (D_s/A) is calculated by eq. (4), when the shape of V_2O_5 sample is spherical or cubic

$$D_s = 6\times10^4/d_s\cdot S \qquad (4)$$

where d_s is the density of V_2O_5 (3.4g/cm^3). D_s-values calculated are shown in Table 3, assuming that d_s-value is constant even if the preparation temperature is changed. D_s-value of **V3** is 5.0×10^3 A which is fairly consistent with the average size (5.2×10^3 A) of the smaller particles estimated from SEM photograph in Fig. 3. Since the molecular diameter of SO_2, which is the reducing agent, is almost same as that of Ar (3.8 A)[9] which is the adsorbate for the BET experiment, it is reasonable to expect that the reaction between V_2O_5 and SO_2 takes place on the surface of smaller particles building up the large particles of V_2O_5.

In order to investigate the influence of the size of larger particles on the reduction rate, two sample powders of different particle sizes (100-150 and 250-325 *mesh*) were obtained by sieving a commercial V_2O_5 (Nakarai Chemical Co., Reagent Grade). The particle structure of the commercial V_2O_5 was found to be similar to that of **V3** from the magnified SEM photograph in Fig. 3. The classification by sieving of prepared V_2O_5 samples was unsuccessful, because the size of large particles was smaller than 10 μm as seen in Fig. 1. The fractional conversions (α) of two groups of commercial V_2O_5 were almost the same; $\alpha=0.16$ and 0.14, respectively, at the reaction temperature of 400 °C and the reaction time of 1 hr. These α-values show that the reduction process is not affected by the size of larger particles. This fact supports the previous expectation that SO_2 gas is supplied sufficiently on the surface of smaller particles and the reduction takes place on them.

According to Hall[10], the peak breadth at half maximum intensity (β_{hoo}) in Table 2 is represented by two terms, that is, the crystallite size (L_a) and the lattice strain of crystallite (η_a) as in the following (eq. (5)).

$$\beta_{hoo}\ cos\theta/K\lambda = 1/L_a + \eta_a\ sin\theta/K\lambda \qquad (5)$$

where λ is the wave length of X-ray, θ is Bragg's angle and K is the shape factor (0.9). L_a

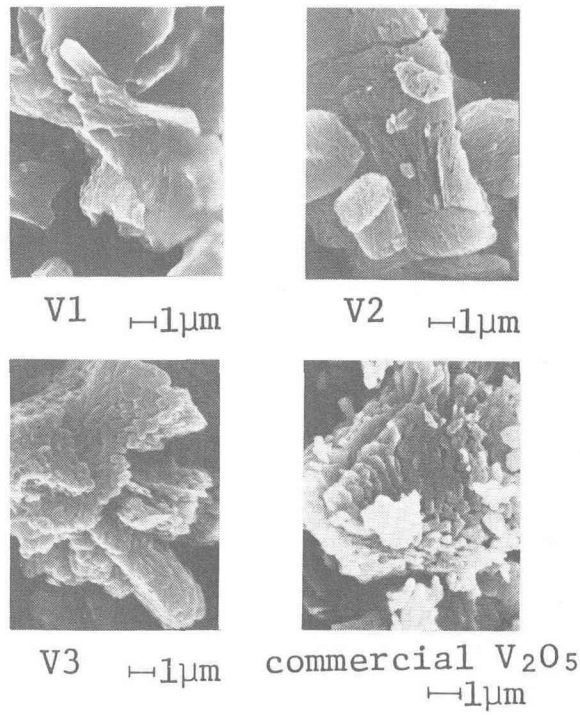

Fig. 3 SEM photographs of V_2O_5 crystallites.

and η_a correspond to the values for the direction of a-axis, because X-ray diffraction peaks were observed for (600), (400) and (200) face. The plot of eq. (5) by using β_{h00}-values in Table 2 give the straight lines as shown in Fig. 4. η_a and L_a obtained are listed in Table 3. The order of η_a is **V1**>**V2**>**V3** and that of L_a is **V3**>**V2**>**V1**. The orders of η_a and L_a indicate that the increase in preparation temperature of V_2O_5 results in the larger crystallite size and the smaller lattice strain; in other words, the increased crystallinity, the higher regularity of crystal lattice and the more uniform size of unit cells which form the crystallites. As seen in Table 2, three samples show similar d_{h00}-values, in contrast to different η_a. Since η_a corresponds to the distribution of interplanar spacing ($<\Delta d/d>$), the calculated value of Δd ($=\eta_a \cdot d_{h00}$), the displacement of (h00) faces, is found to be in the range of $4.1\times10^{-3}\sim12.4\times10^{-3}$ A for **V1**, $1.9\times10^{-3}\sim8.1\times10^{-3}$ A for **V2** and $1.5\times10^{-3}\sim4.6\times10^{-3}$ A for **V3**, respectively. As seen in Table 3, L_a agrees with D_s approximately. Moreover, as described ealier D_s for **V3** also agreed with the average size (5.2×10^3 A) of small particles estimated from SEM photograph in Fig. 3. These agreements in the sizes suggest that the small particle seen in Fig. 3 corresponds to the crystallite of V_2O_5 sample.

As mentioned above, the reduction of V_2O_5 takes place on the surface of its small particles, that is, crystallites and the rate is controlled by the phaseboundary reactions (eq. (3)). The reaction rate for one crystallite is represented by eq. (6),

$$-dw/dt = k_0 sC \qquad (6)$$

where w and s are the weight and the surface area of one crystallite, k_0 is the rate constant and C is the concentration of SO_2 on the surface of the crystallite. When the total weight

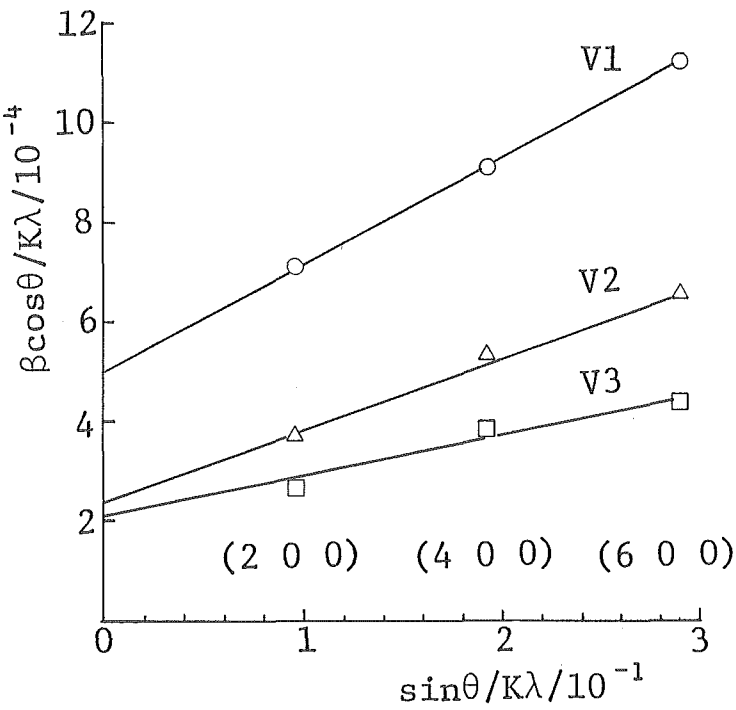

Fig. 4 Hall's plots of V_2O_5 samples.

Table 3 Particle diameter [D_s] calculated from surface area, crystallite size [L_a] and lattice strain [η_a].

Sample	D_s/A	L_a/A	$\eta_a/$
V1	2.4×10^3	2.0×10^3	2.15×10^{-3}
V2	3.2×10^3	4.0×10^3	1.40×10^{-3}
V3	5.0×10^3	4.8×10^3	8.00×10^{-4}

of sample is W, the rate is represented by eq. (7) assuming that the crystallite is cubic and the size is D_s,

$$-dW/dt=(6k_0W_0^{1/3}/d_s\cdot D_s)CW^{2/3} \quad (7)$$

where W_0 is the total weight of the sample before the reaction. Eq. (9) is obtained by integrating eq. (7) and by introducing the fractional conversion (α) in eq. (8).

$$\alpha=1-W/W_0 \quad (8)$$

$$1-(1-\alpha)^{1/3}=(6k_0\cdot C/d_s\cdot D_s)t \quad (9)$$

Then the rate constant k_M of Mampel's equation (eq. (3)) is represented by eq. (10).

$$k_M=6k_0\cdot C/d_s\cdot D_s \quad (10)$$

The density d_s can be assumed to be constant. The value of C is also constant, when SO_2 flow rate is 300 *ml/min*. Thus, it is considered that the difference of k_M in Table 1 is ascribed to that of k_0 and D_s. In order to compare k_0-values for the samples, the value of

$k_M \cdot D_s$ was calculated, which is proportional to k_0. As seen in Table 4, the order of $k_M \cdot D_s$ is **V1>V2>V3** at three reaction temperatures. Since the value of k_0 corresponds to the reaction rate per surface area of the crystallite, it will depend upon the lattice distortion of V^{5+} and O^{2-} or the bond strength between them. It has been reported that the removal of oxygen layer of (020) face plays an important role in the reduction. The IR band of V=O bond(ν) was measured in order to examine the influence of the preparation temperature of V_2O_5 on the bond strength. As seen in Fig. 5, three samples show the absorption spectra at 1020 cm^{-1}, and the difference in ν is not detected among them. On the other hand, the difference could be found in η_a-value which depends upon the degree of the lattice distortion as mentioned above, and its order is consistent with that of k_0-value. Therefore it is

Table 4 $k_M \cdot D_s$ ($\propto k_0$) values of eq. (10).

Sample Reaction temp./°C	$k_M \cdot D_s/A \cdot hr^{-1}$		
	V1	**V2**	**V3**
350	3.26×10	2.94×10	2.80×10
375	7.20×10	6.08×10	5.10×10
400	1.66×10^2	1.25×10^2	1.15×10^2

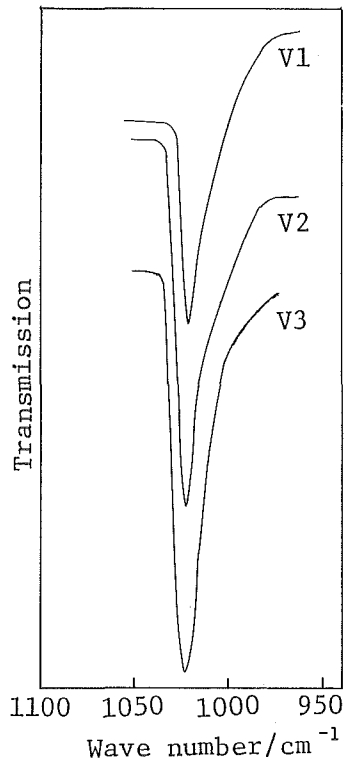

Fig. 5 IR spectra of V_2O_5 samples.

considered that k_0-value depends on the difference in the strain energy accumlating in the samples.

Acknowledgment

The authors are very grateful to Professor T. Morozumi for obtaining the SEM photographs of the samples.

Reference

1) A. Shimizu, R. Furuichi and T. Ishii, J. Chem. Soc. Jap. Chemistry and Industrial Chemistry, **1**, 39 (1975).
2) M. Taniguchi, A. Miyazaki and H. Yokomizo, Catalyst, **10**, 99 (1968).
3) K. Kawashima, K. Kosuge and S. Kachi, Chem. Lett., 1131 (1975).
4) ASTM Card 9-387.
5) ASTM Card 23-724.
6) JIS, G 1221 (1981).
7) S. F. Bartram, "Hand book of X-rays", McGraw-hill (1967) 17-9.
8) K. Mampel, Z. Phys. Chem., **A 187**, 43 (1940).
9) D. W. Breck, "Zeolite Molecular Sieve", John Willy and Sons. (1974) p636.
10) W. H. Hall, Proc. Phys. Soc., **A 62**, 741 (1949).